AD ______________

Award Number: DAMD17-00-1-0599

TITLE: High-Resolution Speckle-Free Ultrasound Imaging System-A Potential Solution for Detecting Missed Breast Cancer

PRINCIPAL INVESTIGATOR: Matthew T. Freedman, M.D.

CONTRACTING ORGANIZATION: Georgetown University Medical Center
Washington, DC 20057

REPORT DATE: October 2004

TYPE OF REPORT: Annual

PREPARED FOR: U.S. Army Medical Research and Materiel Command
Fort Detrick, Maryland 21702-5012

DISTRIBUTION STATEMENT: Approved for Public Release;
Distribution Unlimited

REPORT DOCUMENTATION PAGE

Form Approved
OMB No. 074-0188

1. AGENCY USE ONLY (Leave blank)	2. REPORT DATE	3. REPORT TYPE AND DATES COVERED
	October 2004	Annual (1 Oct 2003 - 30 Sep 2004)

4. TITLE AND SUBTITLE
High-Resolution Speckle-Free Ultrasound Imaging System-A Potential Solution for Detecting Missed Breast Cancer

5. FUNDING NUMBERS
DAMD17-00-1-0599

6. AUTHOR(S)
Matthew T. Freedman, M.D.

7. PERFORMING ORGANIZATION NAME(S) AND ADDRESS(ES)
Georgetown University Medical Center
Washington, DC 20057

E-Mail: Freedmmt@georgetown.edu

8. PERFORMING ORGANIZATION REPORT NUMBER

9. SPONSORING / MONITORING AGENCY NAME(S) AND ADDRESS(ES)
U.S. Army Medical Research and Materiel Command
Fort Detrick, Maryland 21702-5012

10. SPONSORING / MONITORING AGENCY REPORT NUMBER

11. SUPPLEMENTARY NOTES

12a. DISTRIBUTION / AVAILABILITY STATEMENT	12b. DISTRIBUTION CODE
Approved for Public Release; Distribution Unlimited	

13. ABSTRACT (Maximum 200 Words)

The Imperium Inc transmission ultrasound system is a highly promising novel method for imaging the breast. In this pilot project, we are to work with Imperium to advise and help them modify their existing system for non-destructive testing into one suitable for breast imaging, perform a physics evaluation and perform a small clinical pilot feasibility trial. The initiation of this project was delayed by non-approval of the human use portion of the project. We have received US Army Human Use approval for study of tissue samples. We provided technical advice to Imperium, and have performed physics tests and in imaging of pieces of animal tissue obtained in a supermarket.

Imperium has improved the machine during this past year, but the most up to date version is now at the company since it is still under development. Thus we are not ready to start human studies. We have requested approval to image animal tissues since these can be brought to the company and imaged there.

14. SUBJECT TERMS	15. NUMBER OF PAGES
Detection breast cancer, C-Scan ultrasound, CCD coupled Piezoelectric sensor, ultrasound lens	22
	16. PRICE CODE

17. SECURITY CLASSIFICATION OF REPORT	18. SECURITY CLASSIFICATION OF THIS PAGE	19. SECURITY CLASSIFICATION OF ABSTRACT	20. LIMITATION OF ABSTRACT
Unclassified	Unclassified	Unclassified	Unlimited

NSN 7540-01-280-5500

Standard Form 298 (Rev. 2-89)
Prescribed by ANSI Std. Z39-18
298-102

Table of Contents

Cover..**1**

SF 98..**2**

Table of Contents..**3**

Introduction...**4**

Body..**4**

Key Research Accomplishments...**21**

Reportable outcomes...**21**

Conclusions...**22**

References..**22**

Appendices..**None**

High-Resolution Speckle-Free Ultrasound Imaging System--A potential solution for detecting missed beast cancer

Introduction

The Imperium Inc. transmission ultrasound system is a highly promising novel method for imaging the breast. In this pilot project, we are to work with Imperium to advise and help them modify their existing system for non-destructive testing into one suitable for breast imaging, perform a physics evaluation of the system and perform a small clinical pilot feasibility trial. The initiation of this project was delayed by non-approval of the human use portion of the project. We now have approval for work in biopsy specimens and mastectomy specimens. I do not believe the system is ready for human trial and have not proceeded to in vivo studies. We would like to extend the work to include additional animal experiments. As the system has evolved, the best transducers now are placed at Imperium, Inc., rather than at Georgetown and they still need to be further developed before they are ready for human research. Because the company is approximately 30 minutes away by car, animal cadaver experiments appear to be the best way to advance this technology at present.

Body

During the past six months we have used only limited funds while awaiting Imperium's improvements to the machine. We have visited Imperium's R and D site and have worked with the system at Georgetown to learn how the controls operate and to suggest improvements that should be made. The original system used a water bath. This has been supplemented by a dry system in which fluid filled stand-off pads are used to make contact with the artificial tissue under evaluation. We accompanied the company when they had an informal conference with the FDA. This was done to start their learning process of the requirements for eventual FDA approval. Safety information was extensively discussed and there appear to be no safety concerns.

The following represents a combined presentation of work done by Imperium Ltd and Georgetown in testing the system prior to its use in human tissue specimens.

The initial system is a water bath system. A dry system has been constructed and is described later.

The Water Bath System:

To generate real-time images, ultrasound is introduced into the target under study with a large unfocused ultrasound plane wave. The resultant pressure wave strikes the target and is attenuated and scattered. An acoustic lens collects the energy and focuses it onto the ultrasound sensitive array. The array is made up of two components, a silicon detector/readout array and a piezoelectric material that is deposited onto the array through semiconductor processing (see Figure 1). The array is 1 cm on a side consisting of 128×128 pixel elements (16,384) with 85μm pixel spacing. The energy that strikes the piezoelectric material is converted to an analog voltage that is digitized and processed by low cost commercial video electronics.

Note that there is an ultrasound-receiving (piezoelectric) layer deposited onto the chip. A picture of the microarray is shown in Figure 2. The array is responsive over a wide range of ultrasound frequencies, although most imaging is done between 1MHz and 10MHz. The use of a lens provides a simple, inexpensive alternative to complex

beam forming often employed in ultrasound imaging. The user simply focuses by adjusting the lens while looking at the image on a monitor. Figures 3 and 4 show the overall system configuration and the laboratory setting in a water tank, respectively.

The original system operated by pulsing a commercial off-the-shelf ultrasonic spike pulser in 5 MHz frequencies. (In the past three months, the company has been able to improve this system so that it can now produce images up to 10 MHz, providing higher resolution, but with decreased penetration through tissue.) The ultrasound spike pulser excites the large area unfocused ultrasound transducer (only used as a source) and sends an ultrasound plane wave through the water. This plane wave enters the target, scatters, exits the target and strikes the acoustic lens, which collects the scattered energy and focuses it onto the array. This operation repeats 30 times/second to generate real-time image. Standard video electronics and image processing are used to format the image for presentation to the user and perform real time image processing; either on a PC monitor or LCD.

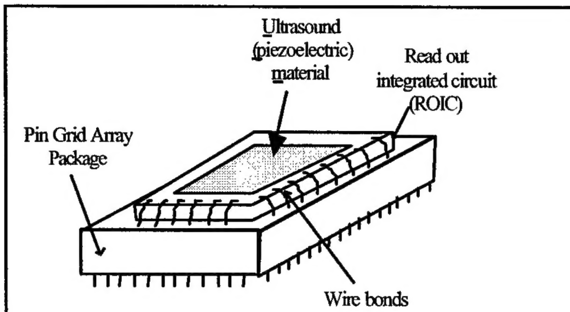

Figure 1. Schematic of array assembled array

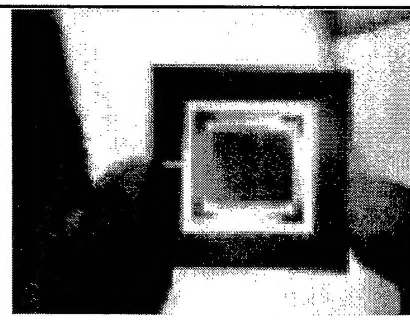
Figure 2. 128 × 128 assembled array

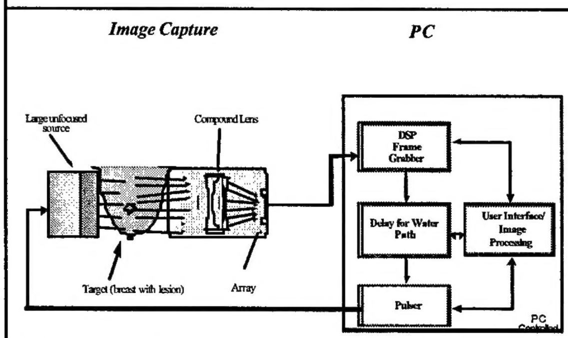

Figure 3. The prototype system configuration

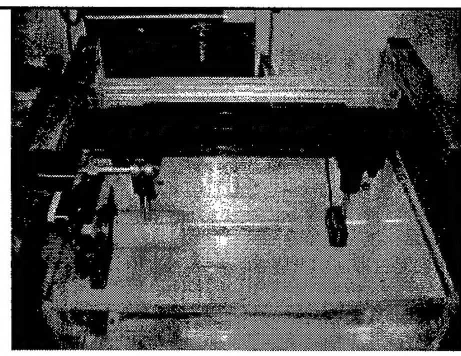
Figure 4. Laboratory setting in a water tank

Contrast Resolution

The ability of the camera to resolve separate tissue layers is a function of its sensitivity to small changes in amplitude. We tested the camera's ability to resolve these small differences in detected signal level. The phantom used in this investigation was a custom-made Zerdine™-based phantom containing 3-mm and 5-mm spheres with small differences in attenuation from the surrounding background material. The phantom was manufactured by Computerized Imaging Reference Systems Inc. (CIRS, Norfolk, VA). The background material has an attenuation of 0.22 dB/cm/MHz that approximates the attenuation of fatty tissue [1, Table 4.6]. Two of the spheres were slightly less attenuating than the background and two of the spheres are slightly more attenuating than the background.

The ability to resolve amplitude differences is measured by calculating a Contrast to Noise Ratio (CNR), given by $CNR = (I_s - I_b) / \sqrt{(\sigma_s^2 + \sigma_b^2)/2}$, where the I_s and I_b are sphere and background mean intensities and σ_s and σ_b are the respective standard deviations. In these measurements, statistics for a block of image pixels inside and outside each sphere area were collected and analyzed. Transmission images were obtained with an Imperium I-100 camera, a two-element aspheric 50 mm diameter F/1 (Imperium 915 series), and a 5.4-MHz center frequency, 1.5 in. diameter pulsed transducer. Figure 5 shows the images taken of this phantom.

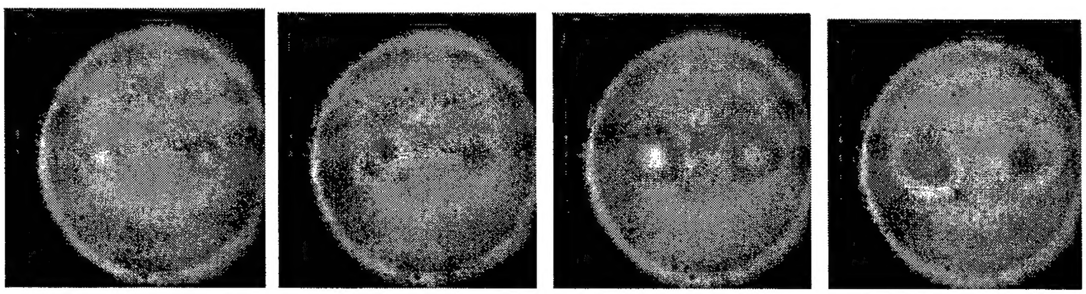

3 mm	3 mm	5 mm	5 mm
0.06dB, 0.15dB	0.5dB, 0.8dB	0.06dB, 0.15dB	0.5dB, 0.8dB

Figure 5 Transmission images of the CIRS contrast phantom.

The sphere diameters and their attenuations (dB/cm/MHz) are indicated in Figure 5. The overall circular field of view indicates the beam diameter. Note the edges around the spheres. The pronounced edges are caused by the refraction edge effect that tends to enhance object resolvability. This effect is known as phase contrast in gapped projection images [2]. We have described this phenomenon and its possible role in enhancing contrast mammography [3]

The results of the CNR calculations are shown in Table 1. Note that there are 256 grayscale levels to represent pixel intensities. This phantom was designed to mimic the breast with embedded cysts and solid masses. The spheres with attenuation less than the background material mimic cysts in this phantom. The spheres with attenuation greater than the background material mimic solid masses.

Table 1
Contrast Resolution

Sphere	**Size (mm)**	**Differential Attenuation (dB)**	**Sphere Mean Intensity**	**Sphere Std. Dev.**	**Back-ground Mean Intensity**	**Back-ground Std. Dev.**	**Contrast**	**CNR**
1	3	0.26	199	17	152	14	47	3.02
2	3	0.12	179	13	152	14	27	2.00
3	3	-0.45	117	11	154	16	-37	-2.69
4	3	-0.94	111	8	154	16	-43	-3.40

Sphere	Size (mm)	Differential Attenuation (dB)	Sphere Mean Intensity	Sphere Std. Dev.	Back-ground Mean Intensity	Back-ground Std. Dev.	Contrast	CNR
5	5	0.44	225	19	149	17	76	4.22
6	5	0.19	166	12	149	17	17	1.16
7	5	-0.75	138	12	157	17	-19	-1.29
8	5	-1.56	99	9	157	17	-58	-4.26

The contrast and CNR calculated in Table 1 must be viewed in the context of the amount of material contributed by the background and by the spheres. The attenuation of the background material is 0.22 dB/cm/MHz, the width of the phantom is 6 cm, and the center frequency of the transducer output is 5.4 MHz. The total attenuation through the phantom where there is no sphere is 7.13 dB. The differential attenuation column indicates the absolute difference between a phantom volume with no sphere and the phantom volume with spheres of different sizes and densities. The differential attenuation column in Table 1 is valid though the center of the sphere. Attenuation through off center sphere volumes will be closer to the background because there is less sphere material. It is notable that objects are resolvable with attenuation differences as small as 0.12 dB.

To determine the relative relevance of this phantom to imaging tissues, we have imaged mouse mammary glands discarded from other experiments because they had not developed tumors.

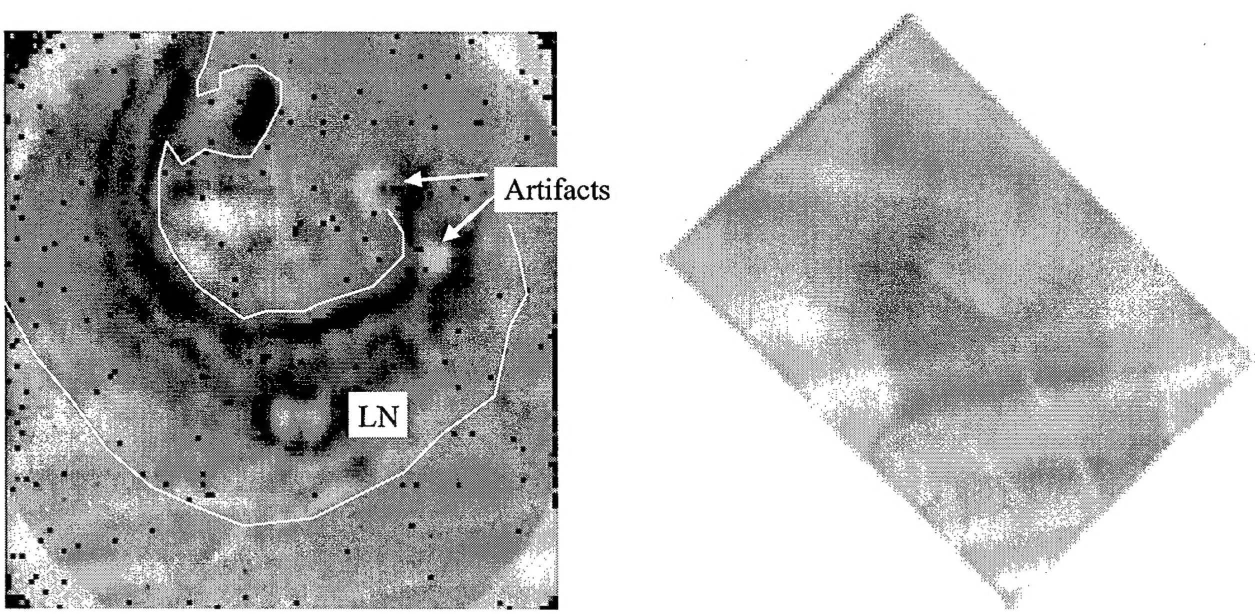

Figure 6. This figure shows an Imperium ultrasound image and a photograph of an isolated mouse mammary gland (gland #4). This gland contains a lymph node (LN) within it that is easily seen on the ultrasound image. In addition, several curvilinear bands are seen within the ultrasound image. On the digital photograph we see vessels within the gland that correspond (most likely) to the light gray band running through the ultrasound image. The Imperium system does not provide measurement capabilities yet, but the overall length of this gland in the mouse is approximately 15 mm. Image was made at 10 MHz. Black dots are defective pixels. This is the first custom-made model of this new ultrasound detector. The lymph node is approximately 2-3 mm in diameter.

Dynamic Range

The dynamic range of the current system is set by the analog output of the camera and the 8-bit analog frame grabber used by the display system. The dynamic range of the next generation camera system is expected to be greater than 70 dB. The next generation camera will incorporate a 14-bit analog/digital converter (ADC) that will preserve the fidelity of the detector array in the accumulation of raw ultrasound data. We expect that the ultrasound data will be compressed to 8-10 bits for video display. Image compression techniques will be used to enhance the contrast resolution of the desired image area. With the use of a variable power output from the ultrasound transducer it is expected that the total dynamic range of the next generation camera will be well over 100 dB.

Twelve images were collected from a custom-fabricated dynamic range step phantom supplied by CIRS. These images are shown in Figure 7. A background pixel intensity of 57 was calculated by observing an area of the display in which there was a de-bonding of the piezo-electric material from the detector array. In this area there is no energy added to the pixel cells from ultrasound detection. Figure 8 shows a graph of pixel intensity versus the attenuation step. Each attenuation step is 2.7 dB.

The images were obtained with an Imperium I-100 camera, a two-element aspheric 50 mm diameter F/1 (Imperium 915 series), a 3.85 MHz center frequency, 1.5" diameter pulsed transducer. The peak sound pressure amplitude output from the transducer was 1.45 MPa.

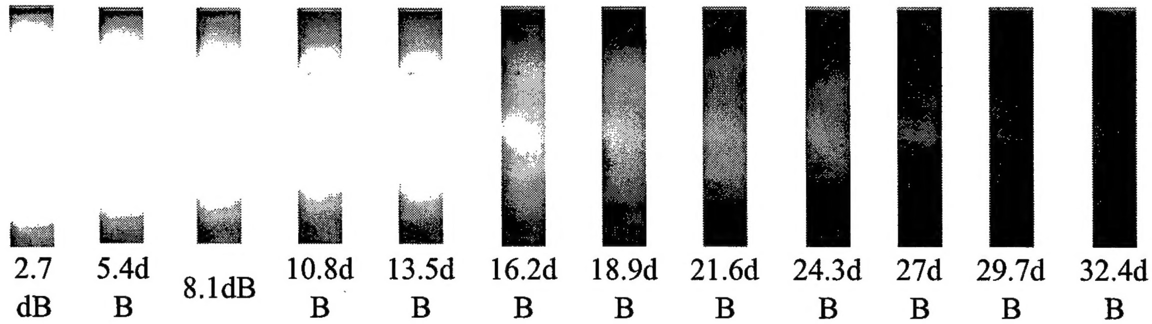

Figure 7. Twelve steps of the dynamic range phantom with associated attenuation @ 3.85 MHz.

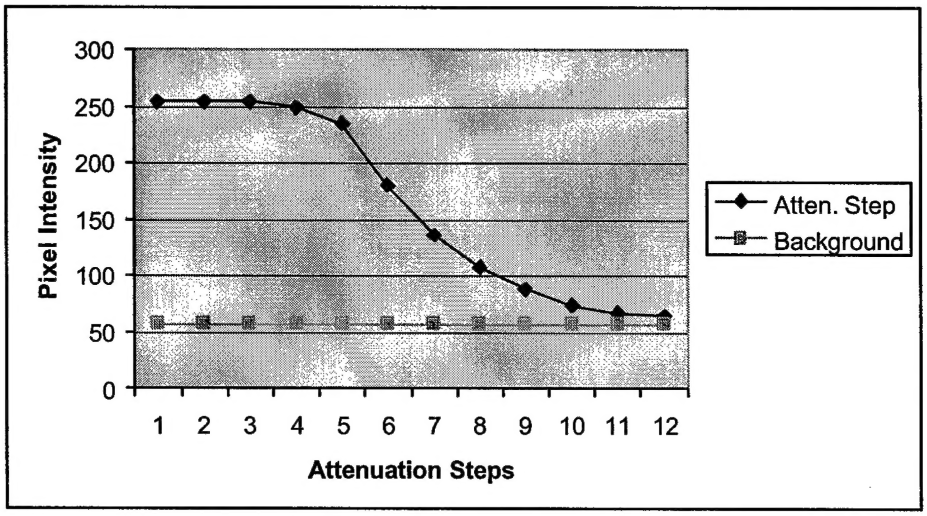

Figure 8 Dynamic Range of I100 Camera. Each attenuation step is 2.7 dB.

As a comment on the dynamic range performance, the camera was able to penetrate 32.4 dB of phantom material. The attenuation of the material at 0.70 dB/cm/MHz approximates that of the average for soft tissue ([1], pg. 51). The phantom is 17.1 cm or 6.84 in. thick at the 32.4 dB step, the current Imperium ultrasound camera should then be capable of penetrating more than 6 in. of soft tissue in its current configuration. Greater sensitivity is expected in the next generation of camera. In mammography, the normal compressed breast thickness varies from 3 to 8 cm depending on breast size and breast density. Thus the dynamic range results support the feasibility of using the Imperium camera for breast imaging (17 cm penetrating ability vs. 8 cm for maximum usual breast thickness).

The newer ultrasound detector has a wider dynamic range and uniformity of response as shown in the figure and table below.

5 MHz	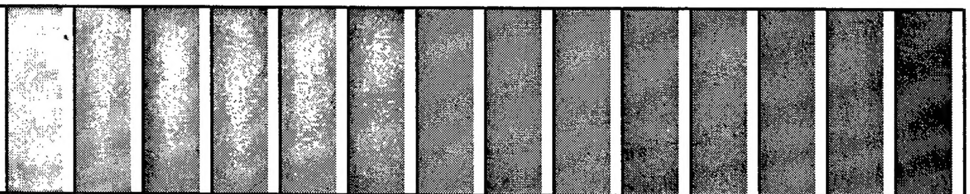													
steps		0dB	4.95	9.9	14.85	19.8	24.75	29.7	34.65	39.6	44.55	49.5	54.45	59.4
Background	0.2	5.4	4.95	4.5	4.05	3.6	3.15	2.7	2.25	1.8	1.35	0.9	0.45	0.
Phantom	0.2	5.4	9.9	14.4	18.9	23.4	27.9	32.4	36.9	41.4	45.9	50.4	54.9	59.4
Total (dB)	**1.88**	**7.08**	**11.58**	**16.08**	**20.58**	**25.08**	**29.58**	**34.08**	**38.58**	**43.08**	**47.58**	**52.08**	**56.58**	**61.08**

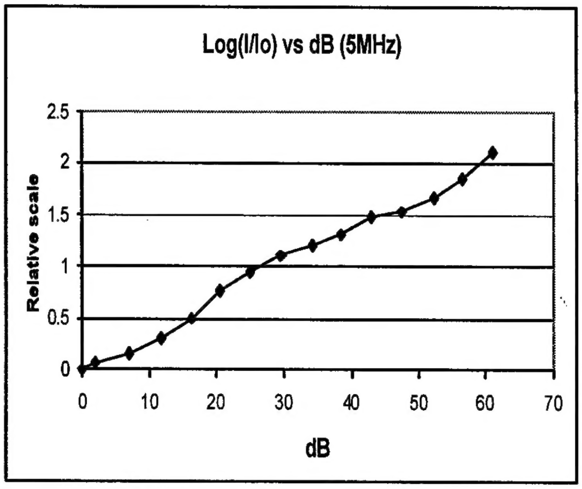

Figure 9: This demonstrates the wider dynamic range of the newly designed and made Imperium camera. This newly designed chip should greatly enhance the detection of abnormalities within breast tissues.

Spatial Resolution

The purpose of this task is to investigate the ability of the camera to resolve separate objects in a field of view, a function of its spatial resolution. The custom-fabricated Zerdine™-based CIRS phantom used in this investigation contains seven, 250 µm steel wires embedded in a fan shape. Transmission image data was obtained with an Imperium I-100 camera, a two-element aspheric 50 mm diameter F/1 (Imperium 915 series), and a 5.4-MHz center frequency, 1.5"-diameter pulsed transducer. Figure 9 shows an image taken of this phantom. Spatial resolution of the camera is determined by its ability to resolve the wires and the gaps between the wires.

The acoustic lenses designed by Imperium for its ultrasound cameras are diffraction limited.
Eq. (1) describes the limit of resolution for the diffraction-limited lens used in this investigation.

$$D_L = 1.22?F/D \qquad \ldots(1)$$

λ = 277 μm (5.4 MHz)
D = diameter of the aperture = diameter of the transducer = 1.5 in. = 3.75 cm
F = Focal Length = 50 mm
D_L = 451 μm

The above computation indicates that the resolution of the system used for this investigation should be about 500 μm. Images shown in Figure 10 and results of work by Ishisaka et al [2] indicate that the phenomenon of phase contrast acts to enhance the edges of objects and may significantly improve the resolution achievable over the limit of Eq. 1.

Quantitative results of the first spatial resolution investigation are shown in Figure 11. The intensity of the steel wires is shown as the lower pixel values and the gaps between the wires are shown as the higher values. The center of the image in Figure 10 is 55 mm from the apex of the fan and the fan spreads at an angle of 4.77°. The distance between the outer two wires at the red line in Figure 10 is 9.17 mm. As can be seen, there is substantial blurring of the wires in the image. The aggregate width of seven, 250 μm wires is only 1.75 mm and so should account for only a small part of the width as seen in the image. The blurring is to be expected as the diameter of the wire is only half the spatial resolution predicted by Eq. 1. Observe that five of the six wire gaps are pronounced and one is obscured. This is due to an imperfection in the phantom. Two of the wires lay on top of each other.

The conclusion from this investigation is that we are limited by the operating frequency of the ultrasound camera. It is desirable that we should be able to resolve the 250 μm wires with no blurring. By doubling the frequency to 10 MHz it is predicted from Eq. 1 that we will be able to image the wires without blurring.

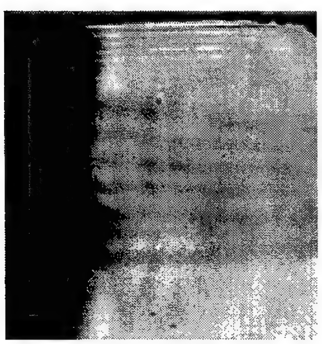

Figure 10 Wire Fan Phantom

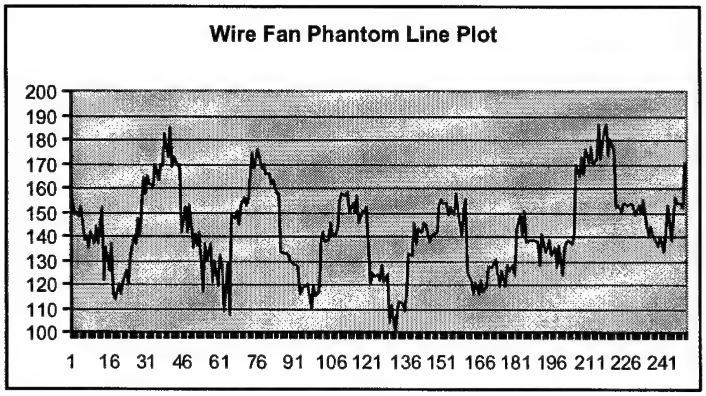

Figure 11 Fan Phantom Line Intensity Plot

A second spatial resolution test was conducted with a CIRS microcalcification phantom. It consisted of Zerdine™ material with imbedded calcium carbonate inclusions with diameters 150-160, 250-280, 320-355, 425-450, and 710-850 μm. Camera images are shown in Figure 12.

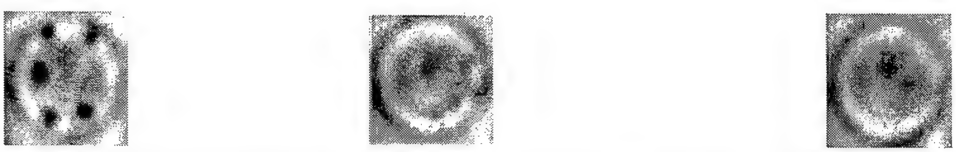

(a)710-850μm target group **(b)**425-450μm target group **(c)**300-355μm target group

Figure 12

Figure 12a clearly shows 700 μm targets. 700 μm is greater than the calculated resolution and thus it is expected that the targets will be easily seen. Figure 12b shows the presence of 450 μm targets but the resolvability of the targets is strained. A single target is clearly seen and other targets are less clearly seen. Unfortunately, most of the targets in this phantom are placed on the lip of an Acrylic dish that holds the targets in place. This is unfortunate because there are refraction effects at the boundaries of this lip that make the targets hard to see. Figure 12c shows the presence of 300 μm targets. The targets in this phantom are blurred as would be expected when the targets are smaller than the resolution limit.

We also evaluated the intensities of the calcification flecks in this phantom. The results are shown in figure 13.

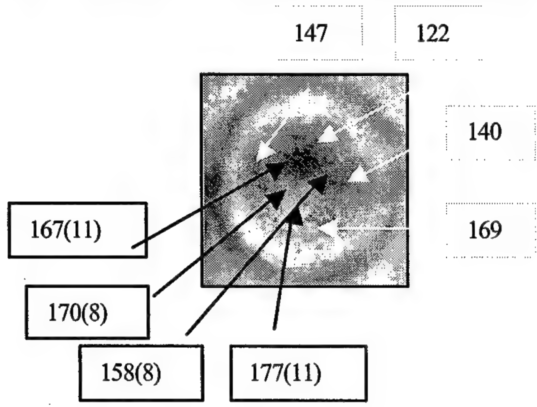

Figure 13: CIRS phantom with calfications ROIs and their intensities and CNRs measures for the smallest clustered calcifications. (A)Four intensity measures for the calcifications upper-right corners and the intensity (noise level) measures at selected background areas

Potential methods to improve resolution

From Eq. 1 it can be seen that resolution can be improved by increasing the frequency, decreasing the focal length, or increasing the diameter of the lens. Decreasing the focal length of the system used in this investigation is impractical. With a lens diameter of 50 mm and a focal length of 50 mm, the current design utilizes a F1 lens. Implementing a smaller focal length would be difficult. Increasing the lens size is possible but there are mechanical limits due to the extended water path. Imperium is currently working on a 3-in. lens design and is investigating the feasibility of a 5 in. lens. One problem with increasing the lens diameter is that the focal length must necessarily increase.

The most practical way to improve resolution is to increase the ultrasound frequency. Eq. 1 is linear, so doubling the frequency to 10 MHz would result in a halving of the resolution to 244 μm. Imperium proposes that increasing the frequency to 13 MHz poses no significant technical problem. The issue in increasing the ultrasound frequency is the increase in attenuation. The tradeoff between increased attenuation and improved resolution will be evaluated in the context of imaging breast tissue. Most conventional B-scan ultrasound systems operate at 12-13 MHz for imaging the human breast so the use of frequencies higher than 10 MHz is likely for the proposed system. Figure 6 shows an early image of mouse mammary gland obtained at 10MHz.

Ultrasound Field and Uniformity

As shown in Figure 14, we have already produced uniform wide-area fields. For a given field size, it has been found that the width of the active area of a pulsed source transducer must be approximately 50 % greater than the desired width of the ultrasound field used for imaging. Thus for a 2" field, a 3" wide transducer is required. The design challenge is the low impedance of such transducers. We used available PiezoCad software to design suitable impedance matching, and we have investigated commercial sources of high-energy pulsers in order to provide wide-field ultrasound with

adequate pressure amplitude for imaging tissue in transmission. We plan to get the adequate source output energy to get a 3 inch square instantaneous field of view for our future medical imaging development.

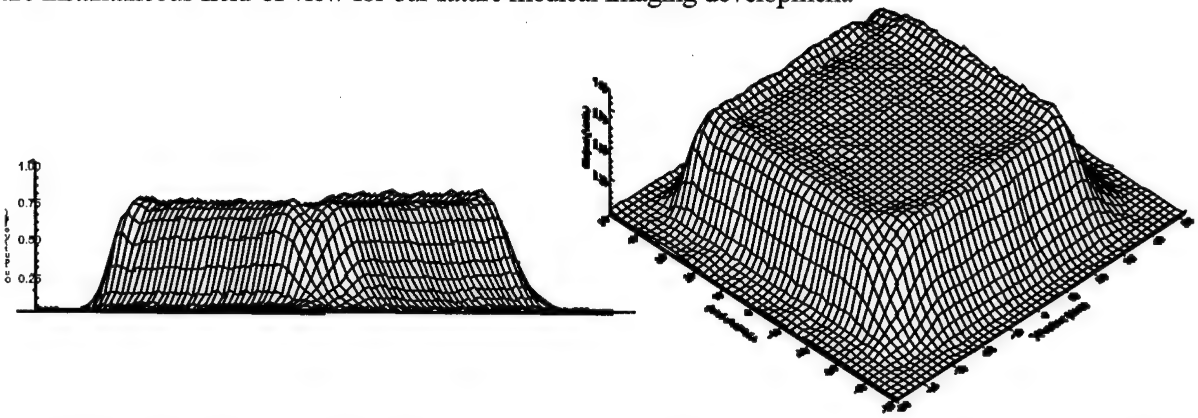

Figure 14: Uniform field from 1.5 MHz Stavely transducer pulsed by Metrotek MP270 pulser and Dapco calibrated hydrophone.

The far field of a transducer is given by the equation:

$$D_{FarField} = \frac{d^2}{4\lambda} \qquad \ldots (1)$$

where $D_{Far\ Field}$ = far field distance, d = transducer aperture, and λ = wavelength

For example, a 0.50 inch transducer operating at 5 MHz will have a wavelength of ≈ 0.012 inches in water, resulting in a far field of ≈ 5.21 inches. Thus all of the data collected with the proposed system will be done within the near field of the transducer.

Imperium engineers have calculated a number of measurements in order to characterize the performance of our transducers. Figure 2 shows a representative series of graphs that show the variation in pressure as a function of transducer aperture position for different distances away from the transducer. This data was collected for a 1.0-inch diameter, 5 MHz transducer. It was measured over a 30 × 30 mm aperture at distances from 0 to 150 mm from the transducer.

Note how the transducer pressure shown in a. is nearly uniform across the aperture with a sharp fall-off at the edges. As the distance from the transducer increases, the aperture shows a distinct lack of uniformity and the edge fall-off is not nearly as pronounced.

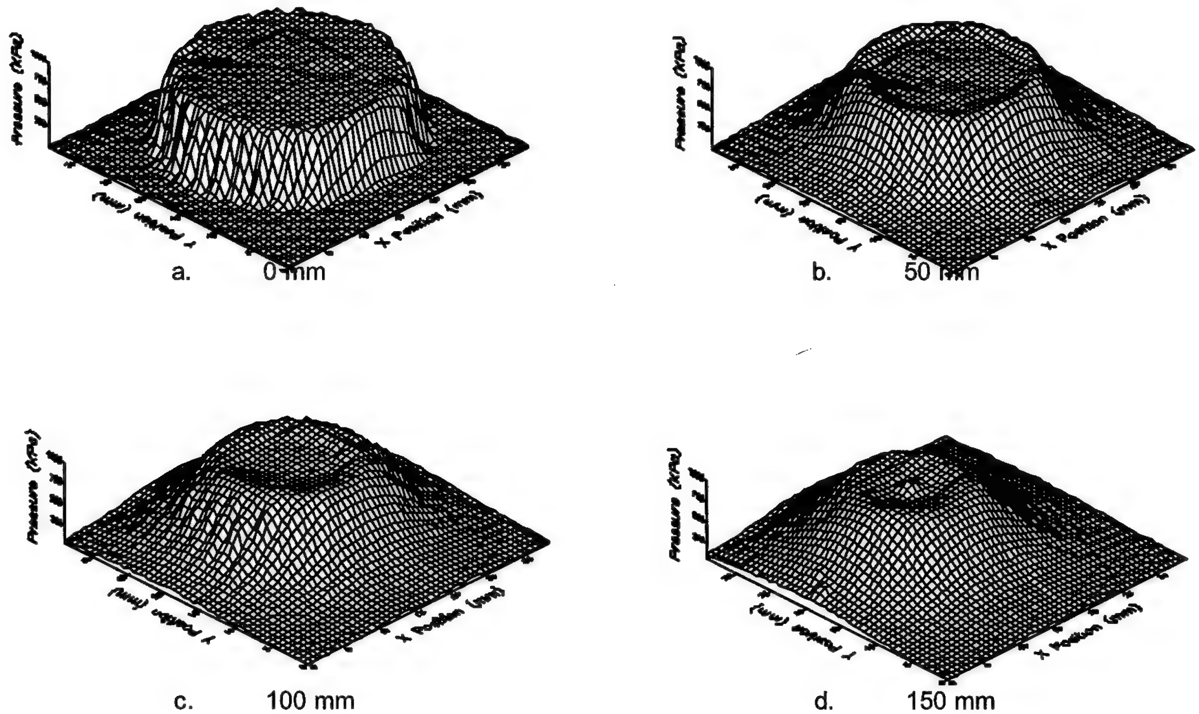

Figure 15 Transducer Pressure Variations with Distance

Zoom Lens Results

The ultrasound imaging system was set up and focused in a manner typically used for imaging with Imperium's ultrasound camera. The transducer was fixed in a position approximately 18 in. from the camera. The two lens elements are Imperium's two-element aspheric 2.75 in. diameter F/1 (Imperium 915 series) lens. Lens elements were moved relative to one another to achieve zoom. The change in image size and the lens positions were recorded. Image size was measured using the AcoustoVision Measurement™ tool (Imperium, Inc.).

Figure 16 shows the relationship of lens movement to image size. Note the monotonic change in image size versus lens change. This relationship is necessary to realize a practical zoom lens design

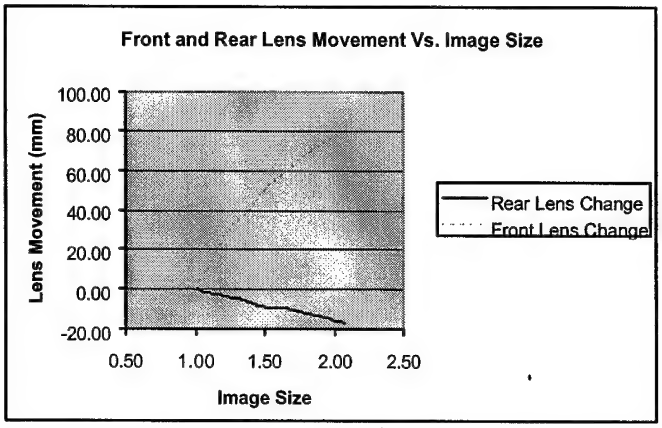

Figure 16 Lens Movement vs. Image Size

A 2:1 zoom was accomplished using a standard lens system by increasing the on-axis distance between the lenses. The front lens moved a distance of 80 mm and the rear lens moved 17 mm from the starting position. The images in Figure 17 show the reference image at the start and end points of the lens positions. Note the enlargement of the 1-in. marks on the ruler in Figure 17b.

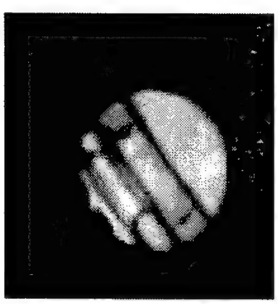

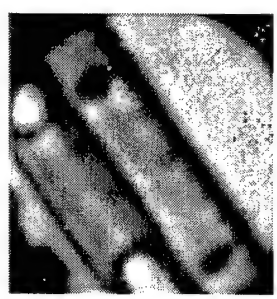

Figure 17a Image With no Magnification **Figure 17b** Magnified Image

Large (3") Field Of View

Two large area-imaging lenses were designed using the Zemax Optical Design Program (Focus Software Inc, Tucson, AZ). Both lens systems are composed of a large diameter objective lens and two smaller focusing elements. The lenses were designed to be diffraction-limited across the surface of the lens. Based on the design in Figure 18, the blur spot size at any given point in the image plane should be no greater than 375 μm for a lens with a three inch diameter, F/1 speed, and an ultrasound frequency of 5.0 MHz. Spot size estimates were performed for several points across the lens surface with the largest spot size occurring at the point farthest from the paraxial axis. The size of the plane wave to be focused and the size of the sensor array determine the magnification of the lens design. In this case, the lens focused a 76.2 mm diameter wave front onto a 10.8 mm square sensor array yielding a magnification of 0.14.

$$m = h' / h = 10.8 \text{ mm} / 76.2 \text{ mm} = 0.14. \qquad \ldots (2)$$

m = magnification
h' = image height
h = object height

The first design consisted of two elements from the Imperium 915 lens with the addition of a third larger diameter objective lens. The working F-number of this design is 1.69 with an estimated off axis blur size of 375 μm. The Zemax Optical design program generated the ray tracing and spot size diagrams shown in Figure 18.

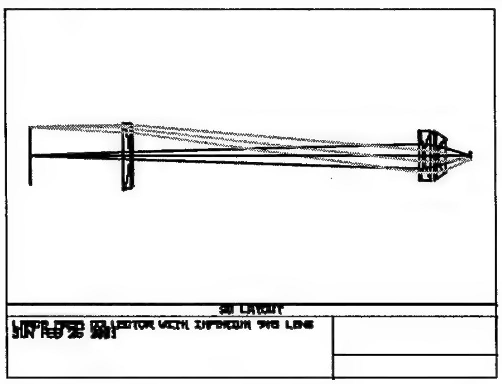

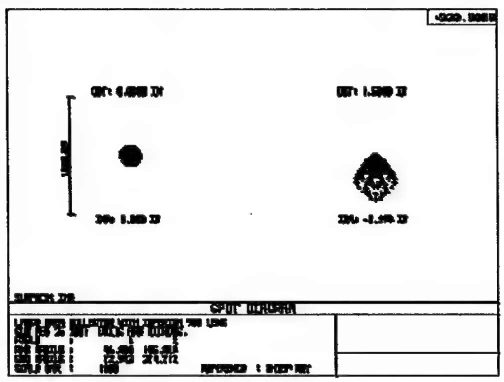

Figure 18a 3-in. Lens, Ray Tracing

Figure 18b 3-in. Lens with 375 micron spot size

A second, improved design is similar but consists of three newly designed lens elements. The working F-number of this design is 1.68 with an estimated off axis blur size of 150 μm. Ray tracing and spot size diagrams of the second design are shown in Figure 19.

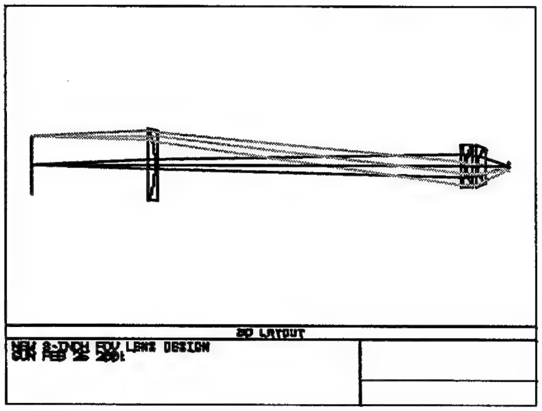

Figure 19a 3-in. Lens, Ray Tracing

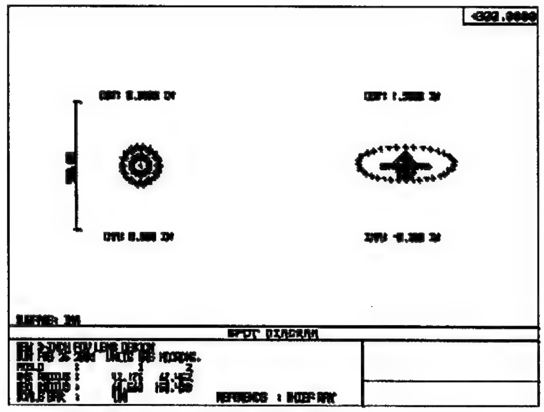

Figure 19b 3-in. Lens with 150 micron spot size

Dry System Implementation

A dry system (no water tank) is required as a practical approach to implementation of a through transmission ultrasound system for medical applications. Imperium has therefore designed and constructed a proof of concept C-arm system in which the ultrasound camera and source transducer are placed on opposing ends of a C-arm mount. The patient is placed between the camera and source for imaging. As discussed in previously, this proof of concept design will serve as a foundation for the fabrication of a clinical breast imaging system. A picture of the prototype dry system is shown in Figure 20.

The C-arm system is designed to provide a means of dry-coupling a patient to an Imperium ultrasound camera in the through-transmission configuration. The system has several degrees of freedom to allow it to move into a convenient position for patient coupling. There are flexible acoustic coupling pads on the transducer and camera sides of the device to provide a comfortable, conformable interface with a variety of irregularly shaped objects. The entire C-arm is mounted to a wheeled cart for added mobility. User interface is accomplished with a standard monitor, keyboard and mouse, along with typical pulser controls.

In testing this system with breast phantoms, it became immediately apparent that when ultrasound coupling gel is used, the system does not adequately fix the breast in place and that the phantom, and therefore a breast, would slide out of the device. Thus modifications of this C-arm system are underway to provide a broader platform to support the breast.

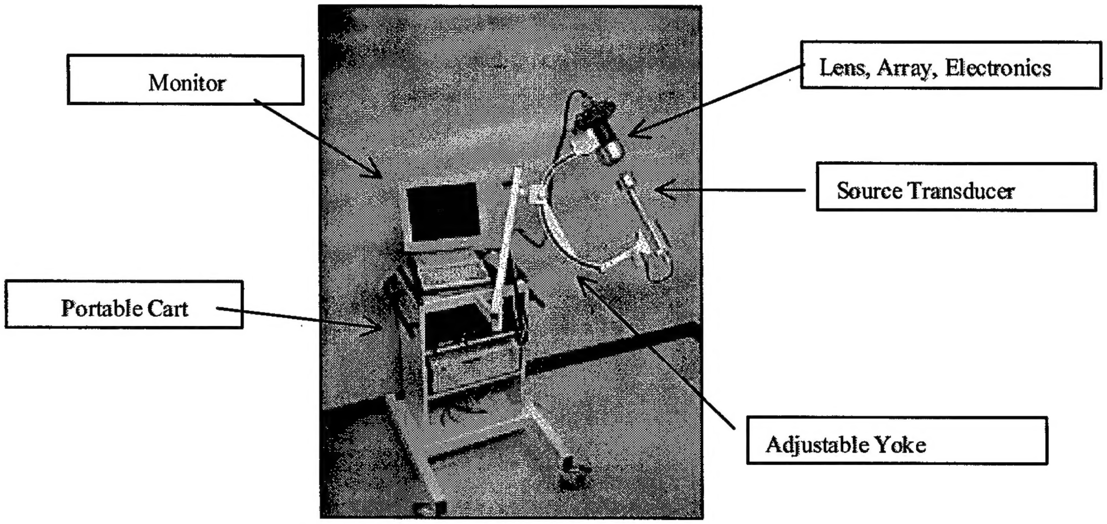

Figure 20 Proof of Concept C-arm System

Improvements in Source Pulsers and Transducers

In order to meet our unique requirements for high-amplitude, wide-area ultrasonic fields, we have designed and built our own small, low-cost, high-voltage pulsers. The pulser design generates a 100 ns pulse with an amplitude variable from 0v to 1 Kv. We will increase the voltage amplitude to 2 Kv. Because of the low impedance of the required high-frequency, large-area source transducers, driving the transducers is difficult with a single pulser driver circuit. We are investigating the use of arrays of multiple smaller transducers each driven by a separate pulser circuit.

An interesting finding is that broadband composite transducers may be detrimental to this application. The lower attenuation at lower frequencies results in loss of spatial resolution. Narrowband ceramic transducers appear to produce a sharper picture. Figures 21a and 21b show the frequency responses of a ceramic and composite transducers respectively. The peaks in Figure 21A are at 4.48 MHz and 5.78 MHz with attenuated low frequency response. The edges of the passband in Figure 21b are at 3.83 MHz and 6.96 MHz.

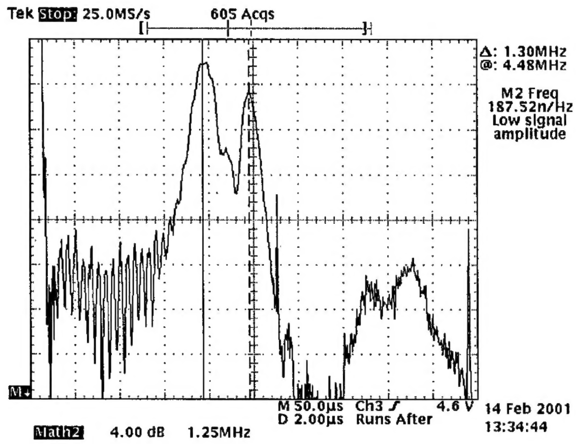

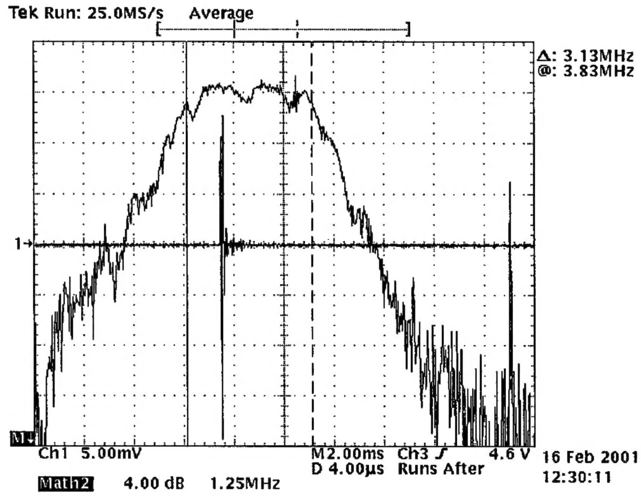

Figure 21a Narrowband Ceramic Transducer **Figure 21b** Broadband Composite Transducer

Simulated Breast Biopsy

To prove the feasibility of using the proposed device in image guided needle biopsy we have performed imaging with a breast phantom. The images in Figures 22a and 22b were taken by Dr. Christopher Merritt of Thomas Jefferson University. The images are of a 1 cm fatty mass with needle embedded in a gelatin phantom. In Figure 22a notice the surface reflection at the bottom of the image, the reverberations from the needle, and the presence of speckle. These are common artifacts of pulse echo ultrasound. Figure 22b which was taken with the through transmission camera from Imperium clearly shows the needle and mass.

Figure 22a Pulse Echo Ultrasound Image
Needle in gelatin phantom

Figure 22b Transmission Ultrasound Image
Needle (white arrow) in phantom next to 1cm mass.

A second set of images (Figure 23) was taken with a CIRS phantom at the Georgetown University Medical Center. Figure 23 shows the sequence of needle biopsy images. The images were sampled from a sequence of 150 ultrasound images taken from 30 frames per second for five seconds. The Imperium ultrasound camera was focused

on two small, simulated masses and a biopsy needle about 4 cm below the surface. The needle first punctured the target (a) and (b), then left (c), and punctured the target again (d) and (e). The needle was rotated clockwise from (e) to (f). This operation pushed the mass on the right upper corner out of the focal plane.

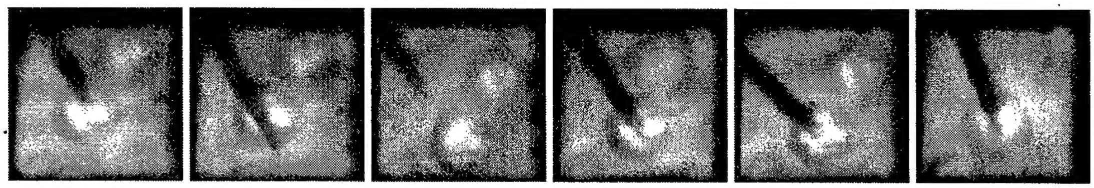

(a) (b) (c) (d) (e) (f)

Figure 23. Needle Biopsy Sequence

In summary, we found the prototype system based on this hybrid microelectronic array that is capable of generating ultrasound images with fluoroscopy-like presentation and without speckle artifacts. The images show no obvious geometrical distortion. The resolution study indicates that a spatial resolution at ~320 microns was observable using a fan-line phantom and calcification phantom. The contrast resolution study indicates that the system is capable of differentiating objects 3mm in size with low differential contrast. The difference between the target and background materials in this experiment was as low as 0.07 dB/cm/MHz.

The potential for use in biopsy procedures is demonstrated through the imaging of breast phantoms with simulated tumors. The system is capable of imaging the area of interest in real-time. In addition, the image resolution and quality generated from the new device seem to outperform over the convertional ultrasound system in terms of inspection of mass spiculation and size of microcalcifications. Clinical investigation of the system is in-progress.

Key Research Accomplishments

We continue to improve our understanding of the parameters of this novel transmission ultrasound system and continue to work with Imperium, Inc on improvements. Improvements have been made in the resolution of the system and in its dynamic range. There is currently only one prototype with the most modern chips and electronics and we will be increasing our activities at the offices of Imperium as we test further. It is currently impractical to image human specimens until we also have the most modern system in our medical facility and so will be imaging animal cadaver tissues as we and the company work to improve the system.

Reportable Outcomes: Publications

Lo SCB, Rich D, Lasser ME, Kula J, Zhao H, Lasser R, and Freedman MT, "A C-Scan Transmission Ultrasound Based on a Hybrid Microelectronic Sensor Array and Its Physical Performance," SPIE Proc. Med. Img. Vol. 4325, 2001.

Liu CC, Lo SCB, Kula J, Rich D, Freedman MT, Lasser R, and Lasser ME "Projection Ultrasound and Ultrasound CT using A CMOS-Based Ultrasound Sensor: A Preliminary Study," SPIE Proc. Med. Img. Vol. 5373 (paper 08), 2004.

Other

One of our graduate students, Chu-Chuan Liu received a Pre-Doctoral Fellowship Award (# DAMD17-01-0197) from the US Army Breast Cancer Program to perform his research on the technical aspects of the Imperium Transmission Ultrasound System. He presented a poster on this at the US Army Breast Cancer Era of Hope Conference in Orlando, FL, Sept 25-28, 2002.

Conclusions

We have seen significant improvement in the design and operating characteristics of the Imperium C-Scan Transmission Ultrasound system. While delays were encountered in start-up, we now have approval to proceed, have worked with Imperium on improvements in the system, and will begin tests on tissue shortly.

References:

[1] McDicken WN, "Diagnostic Ultrasonics" Third Edition, Churchhill Livingstone, 1991

[2] Ishisaka A, Ohara H, and Honda C, " A New Method of Analysis Edge Effect in Phase Contrast imaging with Incoherent X-rays," Optical Review, Vol. 7, No. 6, pp.566-572, 2000.

[3] Freedman MT, Lo S-C.B, Honda C, Makariou E, Sisney G, Pien E, Ohara H, Ishisaka A, Shimada F. Phase Contrast Digital Mammography and Its Clinical Implications. Proc. of SPIE: Physics on Medical Imaging 2003. Paper: 5030-53.